INTERNATIONAL ATOMIC ENERGY AGENCY
UNITED NATIONS EDUCATIONAL, SCIENTIFIC AND CULTURAL ORGANIZATION
INTERNATIONAL CENTRE FOR THEORETICAL PHYSICS
I.C.T.P., P.O. BOX 586, 34100 TRIESTE, ITALY, CABLE: CENTRATOM TRIESTE

H4.SMR/650-5

Workshop on Three-Dimensional Modelling of Seismic Waves Generation Propagation and their Inversion

30 November - 11 December 1992

Lg Coda Q Tomography-- A New Tool for Studying Crustal Structure and Evolution

B. Mitchell

Reinert Professor of Geophysics
Department of Earth & Atmospheric Sciences
Saint Louis University
U.S.A.

Lg Coda Q Tomography --

A New Tool for Studying

Crustal Structure and Evolution

by

Brian J. Mitchell
Reinert Professor of Geophysics
Department of Earth & Atmospheric Sciences
Saint Louis University

Part I

Lg Coda Q - Measurement

and Physical significance

From

Xie, J., and O.W. Nuttli, Interpretation of high-frequency coda at large distances: Stochastic modeling and method of inversion, Geophys. J., 95, 579-595, 1992

and

Xie, J., and B.J. Mitchell, Attenuation of multiphase surface waves in the Basin and Range province, part I: Lg and Lg coda, Geophys. J. Int., 102, 121-137, 1990

1 Introduction

Lg waves observed over continental paths are commonly accompanied by long durations of coda. Since the pioneering work of Aki (1969) on modeling seismic coda as scattered waves, the Lg coda has been utilized to study seismic wave attenuation of continental crust by many authors (*eg.*, Herrmann 1980, Kopnichev 1980, Singh & Herrmann 1983, Raoof & Nuttli 1985, Shin 1985). These results suggest that single station analysis of Lg coda provides a promising means to estimate crustal Q.

We define Lg/fR coda as coda associated with Lg waves which have propagated to distances of 200 km and more. At shorter distnces the coda is mainly associated with shear waves. Several differnces may be seen between these two types of coda. These include the following:

(1) In Lg coda, scattered surface waves seem to dominate, whereas scattered body waves are unlikely to appear due to their geometrical spreading and propagation velocities.

(2) Lg coda has a lower frequency content compared to local coda because of the low-pass effect of anelastic attenuation at large distances.

(3) The possibility of observing multiple scattering in Lg coda should be proportional to epicentral distance. On the other hand, the higher mode surface waves comprising the Lg phase penetrates more deeply (Kennett 1984; Der *et al*, 1984) and are less affected by the presumably stronger scattering caused by near surface heterogeneities. In addition the Lg coda has longer wavelengths due to its lower frequency content and is therefore affected by larger scatterers. The latter factors may well decrease the order of scattering. The dominant order of scattering should be a compromise between the distance effect which increases the order of scattering and these latter effects which decrease it.

(4) The cumulative effect of heterogeneities in the crust encountered by Lg and its coda may cause significant mode conversions. Moreover, the fundamental mode may be excited at shallower depths and arrive at the same time as a portion of Lg coda (Nuttli, 1986). This mode is sensitive to the local geology. In summary, characteristics (1) and (2) make it easier to study Lg coda than local coda, but (3) and (4) make it more difficult.

Despite these complexities, efforts have been made to model Lg coda using stochastic approaches. Kopnichev (1980) proposed a simple model for the joint interpretation of Lg and coda. Der and others(1984), extending the single isotropic scattering model of Sato (1977) (henceforth denoted by "SIS model") to the 2D case, computed Q from the later part of the Lg coda recorded by stations in North America. Consistency was found between the Q values thus obtained and those derived from time domain measurements of Lg. It was also found that the observed relative amplitude level of the coda, compared to that of Lg, was too high to be explained by the SIS model. Factors (3) and (4) above were suggested to be responsible for this discrepancy.

In what follows, I will discuss the effects of the seismic source, dispersion, scattering, and mode conversion on Lg coda and discuss three methods for measuring Lg coda Q.

2 Stochastic modeling of Lg coda

In this paper we assume that the Lg wave is a superposition of higher-mode surface waves with little dispersion; and that the coda of Lg is caused by the scattering and mode conversion of Lg waves. We define the coda travel distance, r, as the total distance traveled by the scattered coda waves. Denoting the lapse time of any part of *Lg* coda by τ and the average group velocity of the Lg wave by V_{Lg}, we have

$$r = V_{Lg}\,\tau . \tag{1}$$

For single scattering, r is the sum of the distances between the seismic source and the scatterer and between the scatterer and receiver. Taking the m^{th} time window centered at lapse time, τ_m, with length T, we assume that the coda wave within this window can be approximated by those scattered Lg waves with a constant coda travel distance, r_m, given by

$$r_m \approx V_{Lg}\,\tau_m , \tag{1-1}$$

provided that the window length T is small compared to τ_m

$$T \ll \tau_m . \tag{2}$$

In previous stochastic models, the statistical mean of coda power spectra has been expressed as the product of terms describing the seismic source, attenuation and scattering. The latter includes a geometrical spreading term which is lapse-time dependent, and a medium term, such as turbidity, which describes the degree of scattering of the medium (*e.g,* Aki & Chouet 1975; Sato 1976).

We now extend this relationship for the mean of coda power (or equivalently, of the coda amplitude spectrum) to the phase spectrum of the dispersive, stochastic Lg coda. By virtue of the convolution theorem this is equivalent to assuming a convolutional relationship in the time series. We assume that the physical process which generates the scattered coda over a constant coda travel distance , r_m , can be described by a time-domain convolution, in which the signal generated by the seismic source is passed through the systems describing the velocity dispersion, geometric spreading, anelastic attenuation, the instrument, and the "medium heterogeneity" of the earth. The latter includes (1) scattering due to those scatterers with a constant coda travel distance r_m and (2) the effects of heterogeneity on Lg modal superposition and mode conversions (Kennett 1984). Thus by sampling the windowed Lg coda at equal intervals Δt , we can express the resulting Lg coda time series $a_{t,m}$ by

$$a_{t,m} = G_m \ (w_{t,m} * s_t * d_{t,m} * \gamma_{t,m} * i_t * n_{t,m}) \quad t = 1,2,\ldots, N_t - 1 \tag{3}$$

where the subscript "t" is an integer whose product with Δt gives the time measured from the beginning of the m^{th} window, "m" stands for the specific window whose center lapse time is given by equation (1-1), "*" denotes the discrete convolution, G_m is the geometric spreading, $w_{t,m}$, s_t , $d_{t,m}$, $\gamma_{t,m}$ and i_t are, respectively, the time series of the window, elastic wave radiation from the seismic source, velocity dispersion, anelastic attenuation, and the recording instrument. $n_{t,m}$ is a time series describing the medium heterogeneity as mentioned above, N_t is the total number of samples in one window, $N_t \ \Delta t = T$.

We define the discrete Fourier transform of (3) as

$$A_{k,m} = \left[\sum_{t=0}^{N_t-1} a_{t,m} \cos\frac{2\pi kt}{N_t} + j \sum_{t=0}^{N_t-1} a_{t,m} \sin\frac{2\pi kt}{N_t} \right] \Delta t \quad k = 0,1,2,\ldots,N_t - 1 \ . \tag{4}$$

Neglecting the window effect and assuming a power law for Lg coda Q, one can apply the discrete convolution theorem to equations (3) and (4) to obtain

$$A_{k,m} = G_m \ [S_k \ D_{k,m} \ \exp(-\frac{\pi f_k^{1-\eta} \tau_m}{Q_0}) \ I_k \ N_{k,m}] \quad k = 0,1,\ldots\ldots,N_t - 1 \ , \tag{5}$$

where capital letters are used for the discrete Fourier transform of the time series in equation (3). Q_0 is Q at 1 hz, η is the frequency dependence of Q, and k is a integer corresponding to a discrete frequency, f_k , through

$$f_k = \frac{k}{T} \ . \tag{6}$$

Another assumption, implied by equation (4), is that the recording site effect can be ignored. As we will see later, this assumption will not affect the resulting Q values obtained with our method, provided that the site effect is statistically stationary. In the following sections, the effects of the different processes expressed in equations (3) and (5) will be discussed in detail.

2.1 DISPERSION

Dispersion, expressed by $d_{t,m}$ in equation (3) and $D_{k,m}$ in equation (5), tends to spread the energy in the coda time series. Denoting the maximum and minimum group velocities of the higher modes comprising Lg by V_{max} and V_{min}, an impulse type of source radiation will have its energy spread over a time length U_m near the coda lapse time τ_m , with

$$U_m = r_m \left(\frac{1}{V_{min}} - \frac{1}{V_{max}} \right) \ . \tag{7}$$

For continental shield regions we take V_{max} to be 3.65 km/sec and V_{min} to be 3.1 km/sec. We assume that the energy spreading due to dispersion is homogeneous within the time duration U_m. If there is no attenuation, the energy spectra of the dispersed source radiation should remain constant by the conservation of energy law. For this case, since the expectation of $S_k^2 D_{k,m}^2 / T$ gives the average distribution of power with frequency (Jenkins & Watts 1965, equation 6.2.1), and since for propagating waves the energy is twice the kinetic energy (Sato 1976, equation (1)), we have

$$W_k = E \left(\rho \omega_k^2 \frac{S_k^2 D_{k,m}^2}{T} U_m \right) \ , \tag{8}$$

where W_k is the statistical mean of the energy spectrum of the source radiation, E stands for the statistical mean or expectation, ρ is the density of the medium and ω_k is the discrete angular frequency.

2.2 GEOMETRICAL SPREADING

The geometrical spreading term, G_m, is perhaps not only the most important, but also the most controversial factor for Q inversion. For local coda that is rich in high frequency content, the validity of the SIS model has been questioned and various alternative models have been proposed (*eg.* Gao *et al.* 1983; Wu 1984; Frankel & Wennerberg, 1987). Unfortunately, only the SIS model is resolvable in single-station Q inversions. Other models introduce additional medium parameters, such as turbidity or scattering Q, which are not well constrained even when more stations are used in inversion.

Sato(1976) first proposed a SIS model for body wave scattering. The extension to the two-dimensional case is outlined in Der *et al.* (1984) and Shin (1985). In Appendix A we have derived the formula in continuous form, and adapted it to the discrete, stochastic form, obtaining

$$G_m = (2\pi R)^{-1/2} \left(\frac{V_{Lg}^2 \tau_m^2}{R^2} - 1 \right)^{-1/4} , \tag{9}$$

where R is epicentral distance, and V_{Lg} and τ_m are defined above.

2.3 RANDOMNESS

The randomness of obeserved coda may be due to many causes, such as the random effects of scattering, mode conversion, velocity dispersion, lateral changes of Q, and irregularity of the seismic sources. In order to express the randomness quantitatively, we introduce spectra $F_{k,m}$ and $W_{k,m}$, which are defined as:

$$F_{k,m}^2 = E\left(S_k^2 D_{k,m}^2 \Gamma_{k,m}^2 N_{k,m}^2 \right) \tag{10}$$

and

$$W_{k,m} = \frac{1}{F_{k,m}} \left(S_k D_{k,m} \Gamma_{k,m} N_{k,m} \right) . \tag{11}$$

It is easy to see that $F_{k,m}$ is deterministic and $W_{k,m}$ is the spectrum of band-limited white noise, since

$$E(W_{k,m}^2) = 1 . \tag{12}$$

$W_{k,m}$ and its inverse discrete Fourier transform, $w_{t,m}$, describe the randomness of coda. Since $w_{t,m}$ is caused by many factors, we can approximate it by Gaussian noise by virtue of the central limit theorem. The effective pass band of coda does not include the DC component, therefore

$$E(w_{t,m}) = 0 . \tag{13}$$

A uniform treatment of coda requires $w_{t,m}$ to be stationary with varying m. If the modeling, especially the geometrical term G_m is reasonable, this requirement should be satisfied.

The last property of $w_{t,m}$ is the independence of spectra $W_{k,m}$'s for different m's. Of all the factors that cause randomness, only the seismic source term remains unchanged when the window number, m changes. If the source effect dominates the randomness, the $W_{k,m}$'s for different m would be dependent. To see if this is the case, we use the fact that the Gaussian character of $w_{t,m}$ will lead to $W_{k,m}$ being Gaussian (Jenkins & Watts 1965). Therefore it is equivalent for $W_{k,m}$ to be uncorrelated or to be independent. We now make use of the common experience that the fluctuations in the source spectral data sets obtained for the same event, but from two well separated stations, are uncorrelated, although the smoothed shapes can be similar. Compared to this situation, spectra of coda from two windows that are separated long enough in lapse time should tend to be less correlated, because of the scattering randomness. Therefore it is reasonable to assume that the $W_{k,m}$'s with different m's are uncorrelated, or independent.

To summarize, the randomness of Lg coda is expressed by $w_{t,m}$, stationary, band-limited white, Gaussian noise with zero mean.

2.4 THE POSSIBLE ROLE OF MODE CONVERSIONS

As mentioned in the discussion of the geometrical spreading term, the SIS model gives a satisfactory geometrical term, but fails to match the observed coda amplitude level relative to the *Lg* amplitude level. Der and his coworkers (1984) suggested that a possible explanation

for this discrepancy is mode conversion.

According to the SIS model, in the absence of mode conversion or any other possible process that could be responsible for the above-mentioned discrepancy, the mathematical expectation of the square of $N^2_{k,m}$ (see equation (5)) would be $2\pi f_k/(V_{Lg}Q_{sc})$, where f_k is the discrete frequency, and Q_{sc} is the scattering Q of the medium. This can modified to incorporate the observed discrepancy, by introducing an empirical spectrum C_k. Then

$$E\left(N^2_{k,m}\right) = \frac{C_k^2 f_k}{Q_{sc}} \quad . \tag{14}$$

For the SIS model without mode conversion, C_k should be of the order of $\sqrt{Q_{sc}}$, because $\sqrt{2\pi/V_{Lg}}$ is very close to one. If C_k is due to mode conversion, it leads to the following two conclusions: First, if dominant conversions occur from higher modes to lower modes (Der *et al.* 1984), where the energy is "packed" into shallower depths, then C_k^2 becomes as big as Q_{sc}. Second, mode conversions must accompany the scattering process, since the *Lg* coda is omni-directional.

3. Method of inversion

3.1 AMPLITUDE DECAY

The most commonly used method in coda Q inversion is that due to Aki & Chouet (1975). In this method, Q's at different frequencies are calculated from the amplitude decay of band-pass filtered coda records. These values are then compared to estimate the frequency dependence of Q. The widths of the filters used in the study of Aki and Chouet (1975) varied from 1.0 hz to 16.0 hz; the frequency resolution is therefore limited to, at best, 1.0 hz. This limited frequency resolution is acceptable for broad-band local coda data.

In the *Lg* coda the total effective pass band is typically narrow (roughly from 0.5 hz to 2.5 hz); this makes it difficult to set a width for band-pass filtering which would give an acceptable trade-off between frequency resolution and variances of Q in each frequency band. This is because we want to keep the frequency resolution as great as possible. It is much better not to separate the coda amplitude spectra at different frequencies, but to

simultaneously fit Q_0 and η over the total effective pass band. In this way only two degrees of freedom are allowed for the Q model through power-law parameterization, while the number of discrete amplitude spectral estimates of coda is kept at a maximum. The variance of this inversion is much easier to control.

3.2 PREDOMINANT FREQUENCIES

Herrmann (1980) proposed a predominant frequency analysis in which Q_0 and η are simultaneously fitted. This method provides a good estimator of Q when coda records with very large lapse times are available, or when the Q is low. In other conditions, the Q estimate is subject to ambiguity, partly because the recorded amplitudes are not used.

3.3 STACKED SPECTRAL RATIOS

In this section we describe a spectral ratio method, which allows us to overcome problems associated with the previous methods. We also describe an extension of the method by which it is possible to invert for the seismic source by jointly using the Lg coda and the direct Lg phase.

First we substitute equations (8), (11) and (14) into (5) to get

$$| A_{k,m} | = \left(\frac{W_k T}{U_m \rho \omega_k^2}\right)^{1/2} \exp\left(-\frac{\pi f_k^{1-\eta}\tau_m}{Q_0}\right) C_k \sqrt{f_k Q_{sc}}\, G_m\, | I_k |\, | W_{k,m} | \quad , \tag{15}$$

where G_m is given in equation (9), $W_{k,m}$ is the discrete Fourier transform of $w_{t,m}$, a stationary, band-limited white, Gaussian noise. Calculating the coda amplitude spectrum from each of two windows of the same length T, but with different center lapse times τ_{m_1} and τ_{m_2} from the same seismogram, we define the scaled logarithmic ratio of the amplitude spectra, R_{k,m_1,m_2} as

$$\begin{aligned} R_{k,m_1,m_2} &= \frac{1}{\pi(\tau_{m_2}-\tau_{m_1})} \log\left(\frac{G_{m_2}\sqrt{U_{m_2}}A_{k,m_1}}{G_{m_1}\sqrt{U_{m_1}}A_{k,m_2}}\right) \\ &= \frac{f_k^{1-\eta}}{Q_0} + \frac{1}{\pi(\tau_{m_2}-\tau_{m_1})} \times \log\left(\frac{| W_{k,m_1} |}{| W_{k,m_2} |}\right) \quad . \end{aligned} \tag{16}$$

The probability distribution function of $| W_{k,m} |$ is of Rayleigh type:

$$P\left(|W_{k,m}|\right) = 2|W_{k,m}|\exp(-|W_{k,m}|^2) , \tag{17}$$

and the theoretical mean and variance of R_{k,m_1,m_2} are

$$E\left(R_{k,m_1,m_2}\right) = f_k^{1-\eta}Q_0 , \tag{18}$$

and

$$VAR\left(R_{k,m_1,m_2}\right) = \frac{1}{12(\tau_{m_2}-\tau_{m_1})^2} . \tag{19}$$

In general, the observational range of η is between 0.0 to 1.0, the order of Q_0 is 10^2 to 10^3, and $\tau_{m_2}-\tau_{m_1}$ is on the order of 10^2 sec. From equation (19), the resulting standard error in R_{k,m_1,m_2} will be of the same order as $f_k^{1-\eta}Q_0$ for frequencies close to 1 Hz. Thus R_{k,m_1,m_2} is an unbiased estimator of $f_k^{1-\eta}Q_0$, but is subject to large standard error. This is a common problem associated with spectral ratios (Aki & Richards 1980, § 11.5.5).

In order to reduce the variance we have designed a two-step procedure. First, we replace A_{k,m_i} by the geometrical mean of the coda amplitude, $<A_{k,m_i}>$, defined by

$$<A_{k,m_i}> = \prod_{i=k-l}^{k+l} |A_{i,m_i}|^{\frac{1}{2l+1}} , \tag{20}$$

where $2l+1$ is the number of points used in each geometrical averaging. The new scaled logarithmic ratio is

$$R_{k,m_1,m_2}' = \frac{1}{\pi(\tau_{m_2}-\tau_{m_1})}\times\log\left(\frac{G_{m_2}\sqrt{U_{m_2}}<A_{k,m_1}>}{G_{m_1}\sqrt{U_{m_1}}<A_{k,m_2}>}\right) . \tag{16-1}$$

Second, we perform a moving-window stack. Since the window length T satisfying equation (2) is normally much shorter than the coda duration, one can obtain many time-shifted windows with their centered lapse times covering the whole coda time series with acceptable signal/noise ratios. For convenience of discussion we assume that there is no overlap of adjacent windows. If there are N_W windows, we define the stacked ratio, F_k, as

$$F_k = \frac{1}{M}\sum_{m=1}^{M} R_{k,m,M+m}' , \tag{21}$$

where M is given by

$$M = \begin{cases} N_W/2 & \text{if } N_W \text{ is even} \\ N_W/2-1 & \text{if } N_W \text{ is odd} \end{cases} .$$

Substituting (16-1) into (21) results in

$$F_k = \frac{1}{M}\sum_{m=1}^{M}\frac{1}{\pi(\tau_{M+m}-\tau_m)}\times\log\left[\frac{G_{M+m}\sqrt{U_m}<A_{k,m}>}{G_m\sqrt{U_{M+m}}<A_{k,m+M}>}\right] . \tag{22}$$

The theoretical mean and variance of F_k are

$$E\left(F_k\right) = \frac{f_k^{1-\eta}}{Q_0} , \tag{23}$$

and

$$VAR\left(F_k\right) = \frac{1}{12(2l+1)M(\tau_{M+m}-\tau_m)^2} . \tag{24}$$

For non-overlapping windows, $\tau_{M+m}-\tau_m = M\times T$ is a constant independent of m. From (23), F_k is an unbiased estimator of $f_k^{1-\eta}Q_0$. From (24) and (19) we can see that by using F_k, the large variance associated to R_{k,m_1,m_2} has been reduced by a factor of $1/M(2l+1)$.

The Q estimation may be done by taking the common logarithm of equation (23):

$$\log_{10}F_k = (1-\eta)\log_{10}f_k - \log_{10}Q_0 + \epsilon , \tag{25}$$

where ϵ represents the random error. Equation (25) defines a standard linear regression problem in which η and $\log_{10}Q_0$ can be estimated. Equation (25) holds when the SIS model is applicable. The effect of seismic sources, mode conversions and the recording site effect will cancel, kprovided thay are stationary processes.

References

Aki, K. & Richards, P.G., 1980. *Quantitative Seismology*, I, W.H. Freeman and Co., San Francisco, California.

Aki, K., 1969. Analysis of the seismic coda of local earthquakes as scattered waves, *J.Geophys.Res.*, 74 , 615-631.

Aki, K. & Chouet, B., 1975. Origin of coda waves: source, attenuation and scattering effects, *J. Geophys.Res.*, 80 , 3322-3342.

Der, Z., Marshall, M.E., O'Donnell,A. & McElfresh T.W., 1984. Spatial coherence structure and attenuation the Lg phase, site effects, and interpretation of the Lg coda, *Bull. Seism. Soc. Am.*, 74 , No.4, 1125-1148.

Frankel, A. & Wennerberg, L., 1987. Energy-flux model of seismic coda: separation of scattering and intrinsic attenuation, *Bull. Seism. Soc. Am.*, 77 , No.4,1123-1151.

Gao, L.S., Biswas, N.N., Lee, L.C. & Aki, K., 1983. Comparison of the effects between single

and multiple scattering on coda waves for local earthquakes, *Bull. Seism. Soc. Am.*, 73 , 373-389.

Herrmann, R.B., 1980. Q estimates using the coda of local earthquakes, *Bull. Seism. Soc. Am.*, 70 , 447-468.

Jenkins, G.M. & Watts, D.G., 1965. *Spectral Analysis and Its Applications*, Holden Day, San Francisco, California.

Kennett, B.L.N.,1984. Guided wave propagation in laterally varying media-I.theoretical development, *Geophys. J. R.astr.Soc.*, 79 , 235-255

Kopnichev, Y.F.,1980. Statistical models for the generation of coda and short-period Lg -phases and the results of their joint interpretation, *Izv.Akad.Nauk USSR.Earth Phys.*, 16 No.2, 99-108.

Nuttli, O.W., 1986. Yield estimates of Nevada test site explosions obtained from seismic Lg waves, *J. Geophy. R.*, 91 No.B2, 2137-2152.

Raoof, M. & Nuttli, O.W., 1985. Attenuation of high-frequency earthquake waves in south America, *PAGEOPH*, 22 , 619-644.

Sato, H.,1976. Energy propagation including scattering effects;single isotropic scattering approximation, *J. Phys. Earth*, 25 , 27-41.

Shin, T-C., 1985. Lg and coda wave studies of eastern Canada, Ph D thesis, St Louis University.

Wu, R.S., 1985. Multiple scattering of seismic waves-separation of scattering effects from intrinsic attenuation-I. Theoretical modeling, *Geophys. J. R.astr.Soc.*, 82 , 57-80.

Part II

A Back-projection Technique for Lg Coda Q Tomography

From

Xie, J., and B. J. Mitchell, A back-projection method for imaging large-scale lateral variations of Lg coda Q with applications to continental Africa, Geophys. J. Int., 100, 161-181, 1990

1 INTRODUCTION

Developments in seismic tomography in recent years have greatly advanced the study of lateral variations of velocity structure in continental areas. By contrast, little progress has been made in imaging lateral variations of Q of the Earth using tomographic algorithms (Nolet 1987). This is largely due to the lack of precision and stability in Q measurements, as well as the lack of a sufficiently large and well-distributed data base.

Vertical-component, high-frequency (~ 1 Hz) Lg waves can be treated as a superposition of higher-mode Rayleigh waves propagating within the continental crust (Knopoff et al. 1973, Der et al. 1984, Kennett 1984). It is reasonable to assume that in the absence of large-scale disruption of the crustal wave guide, Q derived from Lg or its coda is governed by Q in the continental crust. In

this paper we define Lg Q as Q derived from the direct Lg phase and Lg coda Q as Q derived from Lg coda Measuring Lg Q requires either records from two stations on the same great circle path or a record from one station produced by an event for which we have knowledge of the source spectrum (Cheng and Mitchell 1981, Campillo 1987). With data currently available, these requirements will likely result in very poor ray path coverage for studying lateral variations of Q. Lg coda Q can, however, be measured at a single station without knowledge of the source spectrum (Aki and Chouet, 1975; Herrmann, 1980; Xie and Nuttli, 1988); it is therefore more useful than Lg itself for the study of large-scale lateral variations of Q. The interpretation of Lg coda, however, is more difficult than that of Lg. Because high-frequency coda is highly random, it is difficult to model Lg coda properly and regionalized coda Q values resulting from inversion may be characterized by large uncertainties.

In order to improve the precision and stability of Lg codaQ measurements, Xie and Nuttli (1988) proposed a stochastic model for Lg coda. They discussed the effects of various physical processes (eg., dispersion, mode conversions, scattering) which affect the generation of Lg coda. They approximated the randomness of Lg coda by band-limited white, Gausian noise. This approach allows a quantitative estimate of the variance of Q determined by the inversion process. A stacked spectral ratio (henceforth denoted as SSR) method was proposed for Lg codaQ inversion which allows cancellation of station site effects (provided that those effects are stationary) and results in a large reduction of the variance. Improved Q values obtained by the SSR method, plus the rapid evolution of techniques used in seismic tomography, make it possible to develop more quantitative, or computerized, methods to image lateral variations of Lg codaQ, with more rigorous analysis of error and resolution.

2 INVERSE METHODS

As in velocity tomography, the imaging of lateral variations of Lg codaQ proceeds in two steps. First, individual seismograms containing coda are collected and processed to obtain Q values, each being a functional of the distribution of regional Lg Q (or more strictly, of regional Lg codaQ) inside an area sampled by the single-trace coda record. Second, many single-trace measurements are combined to image the lateral variations of Q. A major difference between Lg coda Q tomography and velocity tomography is that the forward modeling involved in the former method must take into account the eliptical region over which scattering occurs whereas the latter considers seismic waves that are restricted to single paths.

§ 2.1 Single-trace measurement of coda Q

High-frequency coda is highly random and the generation of Lg coda involves various complicated physical processes such as scattering, dispersion, mode summation, and mode conversion (Der et al 1984, Snieder 1987, Xie and Nuttli 1988). Consequently, two problems arise in the interpretation of the single-trace coda records. First, because of the randomness of coda it is difficult to obtain a Q estimator which is stable enough to provide an acceptable variance (Der et al. 1984). Second, a coda Q estimator may be subject to systematic deviations from an Lg Q estimator due to imprecise forward modeling. In order to solve these two problems Xie and Nuttli (1988) derived a stochastic model and an inverse method for the interpretation of single-trace Lg coda signals. They used a convolutional relationship to model the processes of Lg coda generation. That relationship allows the effect of those processes to be expressed and examined separately in the frequency domain. In particular, they found that the single isotropic

scattering (SIS) model can satisfactorily explain previous observations on several major continents, and that the randomness of the Lg coda signal can be approximated by simple band-limited white, Gausian noise. The latter approximation allows a quantitative estimation of the theoretical variance of coda Q inversion. Xie and Nuttli found that unacceptably low confidence levels in the Lg coda Q inversion results could occur if a carefully designed variance reduction procedure was not used. At large epicentral distances this problem of low confidence levels can be very serious due to the narrow pass-band of the Q filter. They therefore proposed a stacked spectral ratio (SSR) method to reduce the variance resulting from the inversion. For convenience of discussion we briefly summerize the SSR method in the following paragraphs.

First, the Lg coda time series is divided into a number, N_W, of non-overlapping time windows with a constant window length, T, where the mth window has a centered lapse time τ_m, and $m = 1,2,\ldots, N_W$. For each window of the time series the discrete Fourier transform is performed to obtain the geometrical mean of the amplitude spectrum, $<A_{k,m}>$, at the kth discrete frequency $f_k = k/T$, defined as

$$<A_{k,m}> = \prod_{i=k-l}^{k+l} | A_{i,m} |^{\frac{1}{2l+1}} , \tag{1}$$

where the subscripts i,k represent discrete frequencies, and m denotes the window number. $| A_{i,m} |$ is the ith discrete amplitude spectral estimate obtained by applying the discrete Fourier transform to the mth windowed time series and $2l + 1$ is an integer, which gives the number of amplitude spectral estimates used in each geometrical mean.

The SSR is defined as

$$F_k = \frac{1}{M}\sum_{m=1}^{M}\frac{1}{\pi(\tau_{M+m}-\tau_m)}\log\left[\frac{G_{M+m}\sqrt{U_m}<A_{k,m}>}{G_m\sqrt{U_{M+m}}<A_{k,m+M}>}\right], \tag{2}$$

where M is given by

$$M = \begin{cases} N_W/2 & \text{if } N_W \text{ is even} \\ (N_W+1)/2 & \text{if } N_W \text{ is odd} \end{cases} . \tag{3}$$

U_m is the length of each group velocity window for Lg given by

$$U_m = v\,\tau_m\,(1/v_{min}-1/v_{max}) \tag{4}$$

where v, v_{max} and v_{min} are the average, maximum, and minimum group velocities of the Lg wave train, respectively. G_m is the geometrical spreading term which can be expressed as

$$G_m = \left[\frac{1}{4\pi^2 R\sqrt{v^2\tau_m^2/R^2-1}}\,|_{\tau=\tau_m}\Delta\phi\right]^{-1/2} \tag{5}$$

where $\Delta\phi$ is given by

$$\Delta\phi = \int_{\phi=\phi_1}^{\phi_2} d\phi = \phi_2-\phi_1 . \tag{6}$$

We have replaced the symbol η in Xie and Nuttli (1988) by ϕ in order to avoid confusion with the frequency dependence of Q in equation (7) of this paper. Equation (6) is obtained using equations (A1) through (A5) of Xie and Nuttli (1988) but is more general than equation (A5) because here we have generalized the limits of integration for ϕ. When part of the integration path, which is an ellipse, is missing, the numbers ϕ_1 and ϕ_2 can be found using equation (A4) of Xie and Nuttli (1988). An example of this situation is the case when the ellipse intercepts a continental boundary which is non-transmissive to Lg waves. Otherwise $\Delta\phi$ is 2π and the resulting G_m from equation (5) becomes

$$G_m = (2\pi R)^{-1/2}(v^2\tau_m^2/R^2-1)^{-1/4} . \tag{5'}$$

The right-hand side of equation (2) is calculable from a coda time series.

Assuming a power law for Q

$$Q(f) = Q_0 f^{\eta} , \tag{7}$$

where Q_0 and η are Q at 1 Hz and the frequency dependence of Q, respectively, Xie and Nuttli (1988) used linear regression to find η and Q_0 from

$$\log F_k = (1-\eta)\log f_k - \log Q_0 + \epsilon , \tag{8}$$

where ϵ represents a random error. Both theoretical and observational calculations show that the the SSR provides a statistically stable Q estimator, with the resulting standard error in Q_0 being an order of magnitude smaller than Q_0 itself.

A possible source of major systematic deviations of the Lg codaQ estimator from the Lg Q estimator is the use of an incorrect geometrical spreading term, G_m in equation (2). Using available observations conducted in various areas, including central Asia, North America, and

southern Africa, Xie and Nuttli (1988) made a comparison between the Lg Q_0 and Lg codaQ_0 calculated from applying the single isotropic scattering (SIS) model to digital coda data, and concluded that the geometrical spreading term G_m calculated using the SIS model can be used to calculate the value of Lg codaQ_0 and that that value is close to Lg Q_0 averaged over the same area. These areas have widths of about 10^3 km. This conclusion is semi-empirical and many aspects on the the generation of Lg coda still remain unclear. For instance, we do not yet understand the details of mode conversion, nor why the SIS model appears to be valid. A further complication is that the stochastic modeling of Lg coda may be non-unique (Xie and Nuttli 1988).

§2.2 Spatial interpretation of single trace coda Q measurements

In order to obtain an image of lateral variation of Lg coda Q which closely resembles the lateral variation of Lg Q, one has to interpret single-trace measurements of Lg coda Q in terms of laterally varying Lg Q, ie. one has to make an a priori assumption about how the single-trace measurements of Lg codaQ depend on the laterally varying Lg Q inside the area sampled by Lg coda. >From considerations of the afore-mentioned non-uniqueness in modeling Lg coda and the unclear aspects of Lg coda generation, we think it is premature to assume a detailed, perhaps non-linear, functional relationship of such a dependence to image lateral variation of Lg coda Q. Additional problems in any attempt at using such a detailed functional relationship comes from the tremendous computation time and computer storage involved, and probability of numerical instabilities (Xie and Mitchell, 1988). On the other hand, the Lg coda time series is typically longer than 300 seconds, thus the moving window stacking defined by equation (2) utilizes many windows and results in a stable measurement of Q. Assuming an Lg group velocity of 3.5 km/s and single scattering, the area sampled by the single trace Lg coda will always have a width greater than 10^3 km. This distance is about the same as the widths of the areas over which the consistency between averaged Lg Q_0 and Lg codaQ_0 were observed (§2.1). Therefore we assume that the Lg codaQ obtained by applying the SSR method (with G_m calculated from the SIS model) to a single-trace record of Lg coda gives the

areal average of Lg Q inside the elliptical area corresponding to the maximum τ_m, which will be denoted as τ_{max}, of this record. The major and minor axes of this ellipse are given respectively by

$$a = vt/2 \,|_{t=\tau_{max}} \tag{9}$$

where v is the same as in equation (4), and

$$b = \sqrt{v^2t^2-R^2}\,|_{t=\tau_{max}} \tag{10}$$

(Xie and Nuttli 1988, equations (A3) and (A4). Note that $r_1 + r_2 = vt$ and that the delta function in equation (A3) results in α being equal to vt/R).

Since the τ_{max} of a coda record, under the single-scattering assumption, gives the largest possible area sampled by the Lg coda, the above assumption attributes each coda Q value measured from a single-trace record to the average Lg Q over the largest possible area. We will use this assumption exclusively in imaging lateral variations of Lg coda Q.

It appears that the above assumption will lead to limited resolving power in the imaging of lateral variation of coda Q. Previous practice in determining lateral variations of coda Q (Singh and Herrmann, 1983; Raoof and Nuttli, 1985; Jin and Aki, 1988) have assigned single-trace Q measurements to spatial points, instead of areas. We think that our assumption is more reasonable since high-frequency seismic coda samples an area rather than a spatial point. Moreover, spatial resolution in imaging lateral variations of coda Q is also limited by the random nature of the high-frequency coda signal. This causes more basic and more severe restrictions in resolution compared to any restrictions artificially caused by the assumptions used in our inversion. This basic restriction is very important and profound but has not been addressed previously. We shall give a detailed discussion on this limitation in the following paragraphs.

There is a trade-off between the stability of single-trace coda Q measurements and spatial resolution. As mentioned by Kopnichev (1980), Der et al. (1984) and Xie and Nuttli (1988), the high-frequency Lg coda is highly random. Thus in order to estimate coda Q using spectral ratios, stacking techniques should be used to overcome large variances or uncertainties. Stacking

can be applied either to coda data from repeated paths if they are available, or to coda obtained from many time-shifted windows applied to the same single trace. Moving-window stacking can provide better data coverage since only one record is required for multiple measurements. In this method, as one moves toward later parts of the coda, the area sampled by the signal successively increases and the spatial resolution becomes poorer. This is a special case of the usual trade-off between variance and resolution in inverse problems (Bakus and Gilbert 1970). In measuring coda Q using the master curve method (Herrmann, 1980), better constrained coda Q estimates require use of predominant frequencies measured from the later part of coda, unless Q is very low (Singh and Herrmann 1983, Xie and Nuttli 1988). The method of Aki and Chouet (1975) applies linear regression to amplitudes over lapse time for each of several frequency passbands. More data points are needed in these regressions to reduce the uncertainty in the estimation of slope (which gives Q); thus the later part of coda is also needed in the method of Aki and Chouet. Therefore the randomness of coda is an inherent cause of the limited resolving power of coda Q imaging, regardless of the method used. Compared to this primary limitation in the spatial resolution inherent in narrow-band coda signal, the limitations associated with our assumptions are secondary and probably trivial. At short distances the low-pass effect effect of attenuation is not as serious as it is at large distances where Lg coda is observed; therefore for local S-wave coda recorded by broad-band instruments, the variance could be reduced by increasing $2l+1$ (equation (1)) at the cost of frequency resolution if the SSR method is used, and the trade-off could be set toward a higher spatial resolution.

§ 2.3 Imaging lateral variations of Lg coda Q

In this section we propose a back-projection algorithm to image lateral variations of Lg coda Q. Suppose we have a number (N_d) of Lg coda time series collected from a continental region. We shall denote the Q value calculated by applying the SSR method to the nth time series by $\overline{Q_n}$. We divide the whole area under study into a number of N_g grids with widths of W_{NS} degrees in a north-south direction and W_{EW} degrees in a east-west direction. We parameterize the unknown lateral variation of Lg coda Q by assuming it to be a constant

(Q_m) inside the mth grid. Following the assumption in §2.2, $\overline{Q_n}$ gives the areal average of Lg Q (strickly speaking, Lg coda Q) in the elliptical area sampled by coda waves received at the maximum lapse time, τ_{max}, of the whole time trace. Denoting the area that the nth ellipse overlaps with the mth grid by s_{nm}, we have

$$\frac{1}{\overline{Q_n}} = \frac{1}{S_n}\sum_{m=1}^{N_g}\frac{s_{nm}}{Q_m} + \epsilon_n \quad , n=1,2,\ldots,N_d, \tag{11}$$

where

$$S_n = \sum_{j=1}^{N_g} s_{jn}$$

and ϵ_n is the residual due to the errors in modeling Lg coda and in the Q measurement. Equation (11) is a sparse linear system because many of the s_{nm}'s are zero. We shall use a back-projection, or ART technique (eg., Gordon 1974, Dines and Lytle 1979, McMechan 1983, Suetsugu and Nakanishi 1985, Humphreys and Clayton 1988) to solve equation (11). This technique is an iterative "raw-action" procedure. Our adopted version of this technique to image lateral variation of Lg coda Q is briefly summerized as follows:

(1)calculate s_{nm} for all the (m,n)'s and store all the non-zero s_{nm} values.

(2)construct a starting model for Q_m's, denoted by Q_m^i, for $m=1,2,3,\ldots,N_g$, and i=0 (the superscript i will be used to indicate the last iteration completed over all the coda records).

(3)for each of the n records ($n=1,2,3,\ldots,N_d$), calculate the updated residual Δ_n^i, defined through

$$\Delta_n^i = \frac{S_n}{\overline{Q_n}} - \sum_{m=1}^{N_g}\frac{1}{Q_m^i}s_{nm} \quad . \tag{12}$$

(4)for each of the m grids ($m=1,2,\ldots, N_g$), a new estimate of Q_m, denoted by Q_m^{i+1}, is made by back projecting Δ_n^i into the inverse of the Q_m^i's:

$$\frac{1}{Q_m^{i+1}} = \frac{1}{Q_m^i} + \sum_{n=1}^{N_d}\frac{\Delta_n^i s_{nm}}{\sum_{j=1}^{N_g} s_{jn}^2} \quad . \tag{13}$$

(5)a nine-point spatial smoothing proposed by Suetsugu and Nakanishi (1985) is applied to smooth and stablize the inversion. If we denote the mth grid by $m(l,j)$, where l and j are

grid numbers in the east and north directions, respectively, then the smoothed model $(Q_m^{[i+1]}_{(l,j)})'$ is given by

$$\frac{1}{(Q_m^{[i+1]}_{(l,j)})'} = \frac{1}{29}\left[\frac{1}{Q_m^{[i+1]}_{(l-1,j-1)}}+\frac{1}{Q_m^{[i+1]}_{(l-1,j+1)}}+\frac{1}{Q_m^{[i+1]}_{(l+1,j-1)}}+\frac{1}{Q_m^{[i+1]}_{(l+1,j+1)}}+ +4\left(\frac{1}{Q_m^{[i+1]}_{(l,j-1)}}+\frac{1}{Q_m^{[i+1]}_{(l,j+1)}}+\frac{1}{Q_m^{[i+1]}_{(l-1,j)}}+\frac{1}{Q_m^{[i+1]}_{(l+1,j)}}\right)+\frac{9}{Q_m^{[i+1]}_{(l,j)}}\right]. \quad (14)$$

This smoothing procedure is much like a spatial Gaussian filter, and we have found that unreasonably low (or even negative) Q^{-1} values could result if this smoothing is not applied.

(6)repeat the iterative procedures in (3) through (5) until one of the following criteria is satisfied:

$$i+1 \geq i_{max} , \quad (15)$$

or

$$\frac{\sum_{j=1}^{N_d}(\Delta j^{i+1})^2-\sum_{j=1}^{N_d}(\Delta j)^2}{\sum_{j=1}^{N_d}(\Delta j)^2} \leq \delta^2 \quad (16)$$

where i_{max} is an integer which gives the maximum iteration acceptable and δ is the relative change in the overall residual, or the relative improvement of the degree to which the model fits data. Both numbers were chosen by experience after several tests of the method. Both i_{max} and δ are set before the iteration procedure begins.

The advantages of using back-projection techniques include the minimal computer storage involved, and the rapid convergence achieved. These advantages are very important when an entire continent is being studied. The disadvantage of using this technique is that back-projection does not provide formal estimates of resolution, bias, and error (Suetsugu and Nakanishi 1985). Humphreys and Clayton (1988) suggested using the "point spreading function", which we shall denote as p.s.f., as an approximation of the resolution kernel. To obtain the p.s.f. one simply constructs a model composed of one grid with unit-valued Q^{-1} at the geographic point of interest. The Q^{-1} values in all the other grids are set at zero. Synthetic data using this model are then computed and inverted. The resulting image gives the p.s.f. at this geographic point, which in turn gives a measure of spreading of the resolution

kernel.

The effect of random noise preserved in single-trace Q estimates on the final image can be empirically tested utilizing the sample standard error in $\overline{Q_n}$ due to the randomness of the SSR's (Xie and Nuttli 1988). To do so we denote the standard error associated with $\overline{Q_n}$ by δQ_n, $n=1,2,3,\ldots,N_d$ (note that δQ_n is always positive due to the way standard error is estimated), and assume that δQ_n gives a good measure of the absolute value of real error preserved in the corresponding $\overline{Q_n}$ measurements. We then empirically construct a number, N_d, of noise series, whose nth member have an absolute value equal to δQ_n and a sign that is chosen randomly. The nth term of this noise series is then added to $\overline{Q_n}$ to construct a new set of $\overline{Q_n}$, which we shall denote as

$$\overline{Q_n'} = \overline{Q_n} + \delta Q_n .$$

$\overline{Q_n'}$ values were then inverted to obtain a new Q_m model. The difference between the new image of Q_m values using $\overline{Q_n'}$ and the original image of Q_m values will give us an error estimation for the Q_m values. This process empirically measures the effect of random noise on the Q_m image. The sign of the δQ_n series can be simulated by psuedorandom binary generators in a computer and the process must be repeated several times to obtain an averaged, and more stable error measurement of Q_m values.

§4.2 Imaging lateral variations of η

Imaging the lateral variation of frequency dependence, η, requires another procedure. First, we obtained Q_0 and η for each coda record using the SSR method. This allowed us to calculate single-trace measurements of Q at a frequency other then 1 Hz, say at 3 Hz. These single-trace measurements were then used as $\overline{Q_n}$ in equations (11) and (12) to calculate Q_m values at 3 Hz for each of the m grids, $m=1,2,\ldots,N_g$. Finally, using Q_m for each grid calculated at 1 Hz (§4.1) and 3 Hz and assuming exponential frequency dependence of Q, we calculate η for the same grid using the relationship

$$\eta = \frac{1}{ln\,3}\ln\left[\frac{Q(f)\,|_{f=3Hz}}{Q_0}\right] . \quad (17)$$

It is interesting to compare our resolution in imaging lateral variation in Lg coda Q to the resolution of two-dimensional surface wave velocity tomography. Several authors have conducted studies of lateral variations of long-period surface wave phase and/or group velocities in recent years. Suetsugu and Nakanishi (1985), Montagner (1986), and Hadiouche and Jobert (1988) mapped lateral variations of surface wave dispersion in the Pacific Ocean, the Indian Ocean, and Africa, respectively, using data at periods between a few seconds and a few hundred seconds. In all these studies the spatial resolving power was generally limited to wavelengths of 15 to 20 degrees or more. Resolving power in some cases was locally limited to 40 degrees for situations where the ray coverage was poor (Suetsugu and Nakanishi 1985). Therefore the resolving power in this study using Lg coda waves at frequencies between roughly 0.5 and 2.0 Hz is comparable to that achievable in surface wave tomography at longer periods. This is somewhat surprising since surface wave tomography uses direct paths whereas imaging of lateral variations in the Lg codaQ uses scattered waves, thus requiring smoothing over broader areas. A closer look at this comparison suggested that the resolving power of surface-wave tomography is limited by gaps between ray paths which are typically about 20 degrees. The smoothing techniques used in surface-wave tomography remove these gaps in the inverted velocity image at the cost of resolution. The limitations in resolution in the present study are, however, largely due to the random nature of coda data itself (§2.2). Moreover the Q image may be subjected to greater systematic errors in the single-trace measurements of Q and in their spatial interpretation than are velocity images from surface waves.

The effect of the random error in single trace measurements of Lg coda Q on the image of lateral variations in Q was estimated empirically using the method described in §2.3. Five tests were run to estimate the error in the image of Q_0 and η. In each of the five tests we first constructed two noise, or error series. The absolute values of the nth terms of the first and the second series equal the sample standard errors in Q_0 and η calculated from the nth coda seismogram, respectively. The signs of the nth term of both noise series were randomly generated by a random binary generator. The nth terms of the two noise series were than added to the nth Q_0 and η measurements to construct a new synthetic set of Q_0 and η values. The new sets of synthetic Q_0 and η values were then inverted using the back projection method to obtain Q_0 and η for all of the grids. The differences between the Q_0 and η values for the new image and the original image were then calculated and stored at the end of each test. After all five tests, the absolute values of the five differences in Q_0 and η for each grid were averaged. The averaged values thus obtained gave empirical estimates of absolute error in the imaged Q_0 and η values.

REFERENCES

Aki, K. & Chouet, B., 1975. Origin of coda waves: source, attenuation and scattering effects, *J. Geophys.Res.*, 80 , 3322-3342.

Backus, G. & Gilbert, F., 1970. Uniqueness in the inversion of inaccurate gross earth data, Philos. Trans. R. Soc. London, 266, 123-192.

Campillo, M., 1987. Lg wave propagation in a laterally varying crust and the distribution of the apparent quality factor in central France, J. Geophys. Res., 92, 12,604-12,614.

Cheng, C.C. and Mitchell, B.J., 1981. Crustal Q structure in the United States from multi-mode surface waves, Bull. Seism. Soc. Am., 71, 161-181.

Der, Z., Marshall, M.E., O'Donnell,A. & McElfresh T.W., 1984. Spatial coherence structure and attenuation the Lg phase, site effects, and interpretation of the Lg coda, *Bull. Seism. Soc. Am.*, 74 , 1125-1148.

Dines, K.A. and Lytle, R.J. 1979. Computerized geophysical tomography, Proc. IEEE, 67, 1065-1073.

Gordon, R., 1974. A tutorial on ART, IEEE Trans. on Nuclear Science, NS-21, 78-93.

Herrmann, R.B., 1980. Q estimates using the coda of local earthquakes, *Bull. Seism. Soc. Am.*, 70 , 447-468.

Humphreys E. & Clayton R.W., 1988. Adaptation of back projection tomography to seismic travel time problems, J. Geophys. Res., 93, 1073-1086.

Jin, A. & Aki, K., 1988. Spatial and temporal correlation between coda Q and seismicity in China, Bull. Seism. Soc. Am., 78, 741-769.

Kennett, B.L.N.,1984. Guided wave propagation in laterally varying media-I.Theoretical development, *Geophys. J. R.astr.Soc.*, 79 , 235-255

Knopoff, L., Schwab, F. & Kausel, E.,1973. Interpretation of Lg, Geophys. J. R. astr. Soc., 33,

389-404.

Kopnichev, Y.F.,1980. Statistical models for the generation of coda and short-period Lg -phases and the results of their joint interpretation, *Izv.Akad.Nauk USSR.Earth Phys.*, 16 99-108.

McMechan, G.A., 1983. Seismic tomography in boreholes, Geophys. J. R. astr. Soc., 74, 601-612.

Nolet, G. 1987. Seismic wave propagation and seismic tomography, in: Seismic Tomography with Applications in Global Seismology and Exploration Geophysics., Nolet, G., D. (editor), Reidel Publishing Company, Dordrecht, pp 381.

Raoof, M. & Nuttli, O.W., 1985. Attenuation of high-frequency earthquake waves in south America, *Pure and Appl. Geophys.*, 22 , 619-644.

Singh, S.K. & Herrmann, R.B., 1983. Regionalization of crustal coda Q in the continental United States, *J. Geophys. Res.*, 88 , 527-538.

Sneider, R., 1987. Surface wave holography, in *Seismic Tomography with Applications in Global Seismology and Exploration Geophysics*, Nolet, G. (editor), Reidel Publishing Company, Dordrecht, pp 381.

Suetsugu, D. & Nakanishi, I., 1985. Tomographic inversion and resolution for Rayleigh wave phase velocities in the Pacific Ocean, J. Phys. Earth, 33, 345-368.

Xie, J. & Mitchell, B.J., 1988. Tomographic imaging of large scale lateral variations in Lg coda Q, EOS Trans., 69, 1309.

Xie, J. & Nuttli, O.W., 1988. Interpretation of high-frequency coda at large distances: stochastic modeling and method of inversion, Geophys. J., 95, 579-595.

Part III

Implications of Lg Coda Q for Crustal Structure and Evolution

From

Mitchell, B.J., The frequency dependence of QLg and its relation to crustal anelasticity in the Basin and Range province, Geophys. Res. Lttrs., 18, 621-624, 1991

Mitchell, B.J., Lg coda Q and its frequency dependence in stable continental regions: Implications for crustal structure and evolution (abs), Seism. Soc. Am. (Eastern Section) mtg., Memphis, TN 13-16 Oct. 1991

and

Mitchell, B.J., Seismochronology of the continental crust (abs), Geol. Soc. Am. mtg., Cincinnati, OH, 30 Aug.-5 Sept. 1992

Abstract

Observed Q values for 1-Hz Lg waves which traverse the Basin and Range province exhibit a dependence on frequency which varies as $f^{0.4-0.6}$. By contrast, the frequency dependence of intrinsic Q for shear waves in the crust of the same region is much lower and may be nonexistent. These apparently conflicting observations can be explained by a frequency-independent layered model of shear-wave Q which has very low values in the upper crust and rapidly increasing values at greater depths. The shear-wave Q model which best explains reported values of Q_{Lg} and its frequency dependence consists of an 8-km thick low-Q layer (60 or less) overlying Q values as high as 1000 or more at mid-crustal depths. The low Q_β values in the upper crust are best explained by the presence of fluids in interconnected cracks and pore space. At greater depths, increasing lithostatic pressure closes the cracks, leading to the higher Q_β values. This model also predicts fundamental-mode Rayleigh wave attenuation coefficients which agree with observed values. The result of this study contrasts with that of earlier work in high-Q regions of the eastern United States where shear-wave Q in the upper crust must vary with frequency to explain the observed attenuation of both fundamental-mode Rayleigh waves and Lg.

These results indicate that whereas the frequency-dependence of shear-wave Q is an intrinsic property of crustal material, the frequency dependence of Q_{Lg} arises from both the intrinsic frequency dependence of crustal material and its layered structure. A notation is suggested which distinguishes between the frequency dependence of Q_{Lg} and shear-wave Q.

Introduction

Data that can be used to study the attenuation of the phase Lg and its coda, especially at frequencies near 1 Hz, has increased tremendously in recent years. Observations indicate that Q for these waves varies regionally, being relatively high in old stable regions and relatively low in younger, tectonically active regions (Nuttli, 1973; Singh and Herrmann, 1983; Cong and Mitchell, 1988). Q values for both Lg (Q_{Lg}) and its coda (Q_c) at frequencies near 1 Hz exhibit similar values, being within 10-15% of one another for all regions in the world where both have been determined (Nuttli, 1988). The regional variations of Q_{Lg} and Q_c occur in patterns which vary in the same way as regional variations in crustal shear wave Q (Q_β) in the upper crust obtained from surface wave attenuation studies (Mitchell, 1975; Cheng and Mitchell, 1981; Hwang and Mitchell, 1987). The frequency dependences of Q_{Lg} and Q_c also vary regionally, but in the opposite sense as the Q values; they are lower in stable regions and higher in tectonically active regions (Nuttli, 1988).

Since Lg is a guided wave, controlled predominantly by crustal properties, it can be expected that the regional variation of Q_{Lg} and Q_c and their frequency dependences are caused by lateral changes in the anelastic and scattering properties of crustal rock. Models of Q_β which explain the attenuation of both Lg waves at 1 Hz and fundamental-mode surface waves at intermediate frequencies have been developed for several regions of the world, including the eastern United States (Mitchell, 1980) and western United States (Mitchell, 1981). An important result of those studies is that the frequency dependence of Q_β must be relatively high in the high-Q crust of the central and eastern United States, but is low or non-existent in the low-Q crust of the western United States for frequencies of about 1 Hz and lower. Later work

(Cong and Mitchell, 1988) confirmed the earlier results in North America and showed that the same conclusion also holds for South America and India.

The results described above, that the frequency dependence of Q_{Lg} usually decreases with increasing values of Q_{Lg} whereas the frequency dependence of Q_β increases with increasing Q_β, seem to be contradictory. The main purpose of this paper is to explain that apparent inconsistency. It will be shown that the frequency dependence of Q_{Lg} in the Basin-and Range can be produced by a layered Q_β structure. Thus, frequency dependence of Q_β, such as that which characterizes crustal rocks of the eastern United States, is not required in the Basin and Range. A standard notation will be proposed which distinguishes between the frequency dependence of Q_{Lg}, Q_c, and Q_β.

Observations of Q_{Lg} and Q_c in the Basin-and-Range

Xie and Mitchell (1990) have recently determined Q and its frequency dependence for both Lg and Lg coda waves in the Basin-and-Range province. Using the relation $Q_{Lg}(f) = Q_o f^\eta$, where Q_o is Q_{Lg} at 1 Hz and η is a frequency-dependence exponent, they found that Q_{Lg} can be described by $Q_{Lg}(f) = (267 \pm 56)f^{(0.37\pm0.06)}$ and that Lg coda Q can be described by $Q_c(f) = (275 \pm 26)f^{(0.36\pm0.03)}$ at frequencies between 0.2 and 2.5 Hz. Their determinations utilized a stacked spectral ratio (SSR) method (Xie and Nuttli, 1988) which provides stable determinations of Q with variances which are much smaller than those associated with previously used methods. Singh and Herrmann (1983) obtained $Q_c(f) = (250 \pm 50)f^{(0.45\pm0.05)}$ using a predominant frequency analysis and Chavez and Priestley (1986) obtained $Q_c(f) = (214 \pm 15)f^{(0.54\pm0.09)}$ as average values over a somewhat broader region centered in the Basin-and-Range province.

The similarity of the Q values for Lg waves and coda waves and the similarity of their frequency dependences found by Xie and Mitchell (1990) suggest that Q_{Lg} and Q_c can be used interchangeably when using those waves to infer anelastic properties of the crust or in using the attenuation of one or the other of those waves to measure magnitudes of earthquakes or nuclear explosions from Lg waves, at least in low-Q regions like the Basin-and-Range province. That similarity is particularly convenient when determining crustal models of Q_β which explain Lg attenuation. It means that amplitudes of Lg waves from synthetic seismograms at various distances can be used to determine Q_{Lg} values predicted by crustal models and these can be compared with observed Q_c values which are more abundant than observed Q_{Lg} values.

Implications of the equivalence of Q_{Lg} and Q_c were discussed by Xie and Mitchell (1990). They noted that if the energy flux model of Frankel and Wennerberg (1987) is valid at distances of several hundred to 2000 km in the Basin and Range province the equivalence would suggest that intrinsic Q is the dominant factor affecting wave attenuation there and the effect of scattering Q is much smaller. Very low values of Q_β in the upper crust of the Basin-and-Range have been reported by Cheng and Mitchell (1981), Patton and Taylor (1984), and Lin (1989) from studies of surface waves at intermediate frequencies. Because of the relatively long wavelengths used in the surface wave studies (20 - 150 km) it is likely that those low Q_β values correspond to intrinsic values. Because those Q_β values are so low (50 - 100), it is likely that attenuation over the frequency range 0.2 to 2.5 Hz used by Xie and Mitchell (1990) is also dominated by intrinsic Q effects, as suggested by Frankel and Wennerberg (1987) for the Anza region of southern California. In the following sections, we consequently assume that attenuation at both low frequencies and frequencies near 1 Hz is dominated by intrinsic Q and can be modeled using that assumption.

Crustal Q_β Models for the Basin-and-Range

Crustal Q_β models for the Basin-and-Range province have recently been obtained by Patton and Taylor (1984) and Lin (1989). Although they both exhibit Q_β values which are low compared to models for eastern North America, they differ from one another in the distribution of those values. Q_β^{-1} values for the model of Patton and Taylor (1984) increase continuously from the near surface to upper mantle depths whereas the model of Lin (1989) includes a high-Q zone (low Q_β^{-1}) at depths between about 12 and 25 km (Figure 1). Both models were obtained using the assumption that Q_β is independent of frequency. Frequency-independent models can explain the attenuation of both fundamental-mode surface waves and 1 Hz Lg waves in that region (Mitchell, 1981). Figure 1 also shows a model of the eastern United States (Cong and Mitchell, 1988) which must be frequency dependent in order to explain the attenuation of both fundamental-mode surface waves and Lg.

Differences between the two Basin-and-Range models probably occur because the two studies used different methods to determine the attenuation of surface waves. Patton and Taylor (1984) used the method of Tsai and Aki (1969) which obtains spectral amplitudes at many stations surrounding a seismic event and solves simultaneously for fundamental-mode surface wave attenuation coefficients and the moment of the events. The method is most effective in regions where Q has little lateral variation, but is susceptible to systematic errors, which can give attenuation values which are either too high or too low, depending on path configuration, in regions where Q varies laterally (Yacoub and Mitchell, 1977). Observations by Singh and Herrmann (1983) in the Basin-and-Range indicate that Lg coda Q varies between about 200 and 300 in that region. Thus, the model of Patton and Taylor (1984)

could be biased due to systematic errors in surface wave attenuation determinations.

The model of Lin (1989) was obtained by inverting two-station measurements of both fundamental-mode and first higher-mode Rayleigh waves. Those measurements should give average values even along paths where Q varies laterally. That model includes a high-Q zone at mid-crustal depths. Hough and Anderson (1988), in a study of local earthquake recordings, reported a similar zone of high Q values at somewhat shallower depths (5-12 km) beneath the Anza array in southern California.

The model of Lin (1989) will be used as a starting point for the computations of this study. Three modified forms of his model are used, all of which include a low-Q_β layer with a value of 60 in the upper crust. Stacked spectral ratios are computed for three models, one in which the low-Q layer is 6 km, another 8 km, and another 10 km thick. At greater depths the Q_β values of Lin (1989) are used.

Predicted Values for Q_{Lg}

If attenuation in the Basin-and-Range province is dominated by intrinsic effects, then the attenuation of Lg can be predicted for crustal models which have been determined for that region. In the present study, synthetic seismograms for the Lg phase were computed at several distances for velocity and Q_β models for the crust and upper mantle of the Basin-and-Range and the attenuation of Lg was determined using the stacked spectral ratio (SSR) method of Xie and Nuttli (1988); predicted Lg Q values were thus determined using the same method that was used to obtain observed Q values. The SSR method was applied to synthetic seismograms of Lg computed by mode summation (e.g., Wang, 1981). 20 seismograms were computed over the distance range 300 - 1250 km for Q_β models and velocity models obtained by Patton and Taylor (1984) and Lin (1989). Example seismograms computed at distances between 400 km and 1200 km appear in Figure 2 for the velocity and Q models of Lin (1989). The rapid loss of high frequencies caused by low-Q material in the upper crust is readily apparent.

The solid lines in Figure 3 denote stacked spectral ratios predicted by three modified forms of the model of Lin (1989) in which a low-Q_β surface layer overlies much higher Q_β values at greater depths. The calculated values for those models are compared to observed values of Xie and Mitchell (1990) over the frequency range 0.3 - 3.0 Hz. The best-fitting model is that with an 8 km thick low-Q zone; the SSR for this model is described by the relation $Q_{Lg} = (248 \pm 27)f^{(0.5\pm0.2)}$. The model with a 6 km thick low-Q layer produces higher Q_o and η values and the model with a 10 km thick low-Q layer produces lower values. Results for the model with an 8 km thick layer compare well with the relation $Q_{Lg} = (267 \pm 56)f^{(0.4\pm0.1)}$ obtained by Xie and Mitchell (1990) from stacked spectral ratios of observed Lg waves. The model

also predicts attenuation coefficient values of the fundamental Rayleigh mode at intermediate periods (6 - 35 s) which agree satisfactorily with the observed value of Lin (1989) as shown in Figure 4. The only discrepancy is at a period of 6 s where the predicted value is slightly outside the one standard deviation range of the observations. The model with a 10 km thick low-Q zone predicts values which are in even better agreement in the 6 - 7 s range, whereas the model with the 6 km thick layer predicts values which are substantially lower than observed values. Because it provides the best fit to both Lg and fundamental Rayleigh wave data, the model with an 8 km thick low-Q zone is taken as the best model for this region. The dramatic increase of Q_β at mid-crustal depths is most easily explained as being caused by the closure of cracks due to increasing lithostatic pressure. As suggested by Mitchell (1975, 1980), the low Q_β values in the upper crust imply the presence of fluid-filled cracks and pore space. Reductions in Q due to fluid movement through the crust have been described quantitatively by Mavko and Nur (1975) and O'Connell and Budiansky (1977). Brace and Kohlstedt (1980) summarized the results of Brace (1972) and Brace (1980) indicating that relatively high crustal permeability extends to 8 km and could extend to greater depths. The depth to the high-Q_β zone obtained in this study is therefore consistent with depths commonly associated with enhanced crustal permeability. The dashed line in Figure 3 was produced by the model of Patton and Taylor (1984). The absence of a high-Q layer in that model causes observed Q_{Lg} values and frequency-dependence values to be too low.

The modified Q_β model of Lin (1989) which produced excellent agreement with observed values of Q_{Lg} and its frequency dependence is a frequency-independent model. This result indicates that the frequency dependence of Q_{Lg} near 1 Hz which is observed in the Basin and Range can

be produced by a layered structure in which Q_β increases rapidly with depth at mid-crustal depths. It is possible, however, that Q_β in the deeper portions of the model, particularly the high-Q region, can be frequency dependent. When Q_β is high, resolution of Q_β values is relatively poor, so that frequency dependence cannot easily be detected (Mitchell, 1980).

A high-Q layer was also inferred by Hough and Anderson (1988) using body waves from local earthquakes at frequencies between 15 and 100 Hz for the Anza region in southern California. Their Q_β model consisted of a high-Q layer (> 2000) at depths between 5 and 12 km sandwiched between a 5-km thick surface layer with Q_β values of about 500 and deeper material with Q_β values of about 800. Those values are much higher than those of the present study even though Q_c values there are lower than those of the Basin and Range (Singh and Herrmann, 1983). Their model therefore suggests that crustal Q_β values increase with frequency beginning at frequencies somewhere between 5 Hz and 15 Hz.

The depth range of the high-Q zone in the model of Hough and Anderson (1988) corresponds to the range over which most earthquakes occur in that region. The high-Q zone in the model of Lin (1989) lies between depths of about 12 and 25 km. The depth distribution of earthquakes has been determined in the western Great Basin in a region near the western extent of our region of study (Vetter and Ryall, 1983). The greatest number of earthquakes occur at depths between 10 and 15 km in a zone which overlaps the high-Q zone of the model of Lin (1989), and earthquakes occur in smaller numbers at depths down to the base of the high-Q zone. Thus, it is possible that the depth distribution of earthquakes in the Basin-and-Range province is related to the Q_β distribution there.

A Classification for the Frequency Dependence of Q_{Lg}, Q_c, and Q_β

Expressions for the internal friction (Q^{-1}) of surface waves, assuming that damping losses are small enough that Q^{-2} can be neglected, were given by Anderson *et al.* (1965). The equation for Rayleigh waves is

$$Q_R^{-1}(\omega) = \sum_{l=1}^{L} \left(\left(\frac{\beta_l}{C_R} \frac{\partial C_R}{\partial \beta_l} \right)_{\omega\alpha} Q_{\beta l}^{-1} + \left(\frac{\alpha_l}{C_R} \frac{\partial C_R}{\partial \alpha_l} \right)_{\omega\beta} Q_{\alpha l}^{-1} \right) \qquad (1)$$

where the subscript l is the layer index, the subscripts R, α and β identify Rayleigh, compressional, and shear waves, respectively, ω is angular frequency, and C_R is Rayleigh wave phase velocity. The subscripts ω, α, and β indicate that those quantities are held constant when the partial derivatives are computed.

This equation can be used to calculate Q_R^{-1} for any Rayleigh mode by using the appropriate velocities, partial derivatives, and intrinsic Q values. Mitchell (1980) extended this expression to incorporate shear-wave Q values which vary with frequency as

$$Q_{\beta l}(f) = C_l f^{\zeta} \qquad (2)$$

where ζ is an exponent which describes the frequency dependence of Q_β. Nuttli (1986) assumed that the frequency dependence described by Mitchell (1980) for Q_β also pertained to Q_{Lg}. However, equations (1) and (2) indicate that frequency dependence of Q_R^{-1} can be caused either by frequency-dependent Q_β in the crust or by an appropriately layered structure in which Q_β is independent of frequency. Results of the present study indicate that the layered structure in the Basin and Range causes Q_{Lg} to increase with frequency. That increase occurs because higher frequencies include a greater number of higher modes than low frequencies and those higher-order modes sample more deeply in the crust than lower order modes. A high-Q lower

crust will therefore produce a positive frequency dependence of Q_{Lg}. Thus, the frequency dependence of Q_{Lg} and Q_β should be described by two different parameters. I therefore propose that the frequency dependence of the attenuation of Lg waves be described by the parameter η and that the frequency dependence of internal friction for shear waves be described by the parameter ζ. Q_{Lg} would then be described by

$$Q_{Lg}(f) = Q_o f^{\eta}. \qquad (3)$$

If the crust and upper mantle were comprised of flat layers with laterally uniform elastic and anelastic properties, equations (1) and (2) could provide a good approximation for the effect of anelasticity on the attenuation of Lg waves which, as indicated by equation (3), may have a different frequency dependence. It is known, however, that heterogeneities distributed throughout the lithosphere produce a long coda following the Lg wave which cannot be replicated in synthetic seismograms computed for plane-layered structures (Aki and Chouet, 1975). Since the Lg coda is composed of scattered waves which travel longer paths than that taken by Lg, it appears that the frequency dependence of the attenuation of Lg coda should be described by yet a third parameter which I tentatively designate η'. Then

$$Q_c(f) = Q_o' f^{\eta'}. \qquad (4)$$

In low-Q regions, such as the Basin-and-Range, it appears that very low intrinsic Q material in the crust attenuates scattered waves at the same rate as it attenuates the direct Lg wave. Thus the relations $Q_o' = Q_o$ and $\eta' = \eta$ may be appropriate for all low-Q regions. Further work, using methods capable of providing stable measurements of Q_{Lg} and Q_c and their frequency dependences, will be necessary in high-Q regions to see if the relations $Q_o' = Q_o$ and $\eta' = \eta$ hold everywhere.

Conclusions

All of the frequency dependence of Q_{Lg} in the Basin and Range province can be explained by a layered frequency-independent model in which Q_β increases rapidly with depth from very low values (< 100) in the upper 8 km of the crust to high values at greater depths. It is possible that the high-Q layer is frequency dependent, but that that dependence cannot be detected because of poor resolution in high-Q material. The change from low to high values of Q_β most likely occurs because of the closure of cracks produced by increasing lithostatic pressure with depth. The frequency independence of this model contrasts with results from the central and eastern United States where frequency dependence of Q_β in the upper crust is required to explain the attenuation of both fundamental-mode Rayleigh waves and Lg waves.

Frequency dependence of Q_{Lg} and its coda at frequencies near 1 Hz can therefore be caused by at least two factors, by layering in a frequency-independent Q_β model or by an intrinsic frequency dependence of Q_β. It is likely that both factors will prevail in many regions. The frequency dependence (η) of Q_{Lg} and the frequency dependence (ζ) of Q_β are thus fundamentally different parameters and can differ greatly from one another. The frequency dependence (η') of Q_c may, in general, be different from both η and ζ, but in the Basin and Range, at least it appears that $\eta = \eta'$, at least near 1 Hz. Since that equivalence occurs because of the rapid attenuation of scattered waves, it is likely that $\eta = \eta'$ in other low-Q regions. Further work is necessary to ascertain whether or not this is also true of high-Q regions.

Acknowledgment

I am grateful to Jia-kang Xie for providing his program for computing stacked spectral ratio values and to Wen-jack Lin who provided the Q model for the Basin-and-Range province used in this paper. The program for computing the synthetic seismograms used for the theoretical stacked spectral ratios was written by C.Y. Wang and R.B. Herrmann. This research was supported by the Advanced Research Projects Agency of the Department of Defense and was monitored by the Geophysics Laboratory under contract F19628-87-K-0036.

References

Aki, K., and B. Chouet, Origin of coda waves: source, attenuation, and scattering effects, *J. Geophys. Res.*, *80*, 3322-3342, 1975.

Anderson, D.L., A. Ben-Menahem, and C.B. Archambeau, Attenuation of seismic energy in the upper mantle, *J. Geophys. Res.*, *70*, 1441-1448, 1965.

Brace, W.F., Pore pressure in geophysics, in *Flow and Fracture of Rocks, Geophys. Mono. Ser.*, *16*, edited by H.C. Heard, I.Y. Borg, N.L. Carter, and C.B. Raleigh, 265-273, AGU, Washington, DC, 1972.

Brace, W.F., Permeability of crystalline and orgillaceous rocks, *Int. J. Rock Mech. Min. Sci.*, *17*, 241-251, 1980.

Brace, W.F., and D.L. Kohlstedt, Limits on lithospheric stress imposed by laboratory experiments, *J. Geophys. Res.*, *85*, 6248-6252, 1980.

Cheng, C.C., and B.J. Mitchell, Crustal Q structure in the United States from multi-mode surface waves, *Bull. Seism. Soc. Am.*, *71*, 161-181, 1981.

Cong, L., and B.J. Mitchell, Frequency dependence of crustal Q_β in stable and tectonically active regions, *PAGEOPH*, *127*, 581-605, 1988.

Frankel, A., and L. Wennerberg, Energy-flux model for seismic coda: separation of scattering and intrinsic attenuation, *Bull. Seism. Soc. Am.*, *77*, 1223-1251, 1987.

Hough, S.E., and J.G. Anderson, High-frequency spectra observed at Anza, California: Implications for Q structure, *Bull. Seism. Soc. Am.*, *78*, 692-707, 1988.

Hwang, H.J., and B.J. Mitchell, Shear velocities, Q_β, and the frequency dependence of Q_β in stable and tectonically active regions from surface wave observations, *Geophys. J. Roy. Ast. Soc.*, *90*, 575-613, 1987.

Lin, W.J., Rayleigh Wave Attenuation in the Basin and Range Province, M.S. Thesis, Saint Louis University, 55 pp., 1989.

Mavko, G.M., and A. Nur, Melt squirt in the asthenosphere, *J. Geophys. Res.*, *80*, 1444-1447, 1975.

Mitchell, B.J., Regional Rayleigh wave attenuation in North America, *J. Geophys. Res.*, *80*, 4904-4916, 1975.

Mitchell, B.J., Frequency dependence of shear wave internal friction in the continental crust of eastern North America, *J. Geophys. Res.*, *85*, 5212-5218, 1980.

Mitchell, B.J., Regional variation and frequency dependence of Q in the crust of the United States, *Bull. Seism. Soc. Am.*, *78*, 1531-1538, 1981.

Nuttli, O.W., Seismic wave attenuation and magnitude relations for eastern North America, *J. Geophys. Res.*, *78*, 876-885, 1973.

Nuttli, O.W., Yield estimates of Nevada Test Site explosions obtained from seismic Lg waves, *J. Geophys. Res.*, *91*, 2137-2151, 1986.

Nuttli, O.W., Lg magnitudes and yield estimates for underground Novaya Zemlya nuclear explosions, *Bull. Seism. Soc. Am.*, *78*, 873-884, 1988.

O'Connell, R.J., and B. Budiansky, Viscoelastic properties of fluid-saturated cracked solids, *J. Geophys. Res.*, *82*, 5719-5735, 1977.

Patton, H.J., and S.R. Taylor, Q structure of the Basin and Range from surface waves, *J. Geophys. Res.*, *89*, 6929-6940, 1984.

Singh, S.K., and R.B. Herrmann, Regionalization of crustal coda Q in the continental United States, *J. Geophys. Res.*, *88*, 527-538, 1983.

Tsai, Y.B., and K. Aki, Simultaneous determination of the seismic moment and attenuation of seismic surface waves, *Bull. Seism. Soc. Am.*, *59*, 275-287, 1969.

Vetter, U.R., and A.S. Ryall, Systematic change of focal mechanism with depth in the western Great Basin, *J. Geophys. Res.*, *88*, 8237-8250, 1983.

Wang, C.Y., Wave Theory for Seismogram Synthesis, Ph.D. Dissertation, Saint Louis University, 235 pp., 1981.

Xie, J., and B.J. Mitchell, Attenuation of multiphase surface waves in the Basin and Range province, Part I: Lg and Lg coda, *Geophys. J. Int.*, in press, 1990.

Xie, J., and O.W. Nuttli, Interpretation of high-frequency coda at large distances: stochastic modelling and method of inversion, *Geophys. J.*, *95*, 579-595, 1988.

Yacoub, N.K., and B.J. Mitchell, Attenuation of Rayleigh wave amplitudes across Eurasia, *Bull. Seism. Soc. Am.*, *67*, 751-769, 1977.

Figure Captions

Figure 1. Models of Q_β^{-1} obtained from surface wave attenuation. The solid lines indicate a frequency-dependent model for the eastern United States for which Q_β varies as $f^{0.5}$ (Cong and Mitchell, 1988). The dashed line is a frequency-independent model for the Basin-and-Range province. Both models explain the attenuation of fundamental-mode surface waves and 1-Hz Lg waves in the regions they represent.

Figure 2. Synthetic Lg seismograms computed by model summation (Wang, 1981) for distances between 400 and 1200 km. The seismograms were computed for along an azimuth of 45° from a vertical strike-slip fault at a depth of 5 km and oriented in a north-south direction. Seismograms were computed at 20 distances and stacked to obtain stacked spectral ratios using the method of Xie and Nuttli (1988). The time scale is reduced at each distance R using a reduction velocity of 5.0 km/s.

Figure 3. Stacked spectral ratios (circles) obtained by Xie and Mitchell (1990) for the Basin-and-Range province over frequencies between 0.3 and 3.0 hz. A least squares fit to this data gives $Q_{Lg} = (267 \pm 56)f^{(0.4\pm0.1)}$. The solid lines represent theoretically predicted values for modified versions of the model of Lin (1989) in which the upper crust is assigned a Q_β value of 60 and allowed to vary in thickness between 6 and 10 km. The dashed line represents theoretically predicted values for the model of Patton and Taylor (1984).

Figure 4. Attenuation coefficient values observed by Lin (1989) in the Basin and Range province. Vertical bars denote one standard deviation. Solid lines indicate values predicted by the Q_β model of the lower crust and

upper mantle in Figure 1 combined with an upper crust with a Q_β of 60. The thickness of that upper crustal layer varies, being 6, 8, and 10 km thick for three computations.

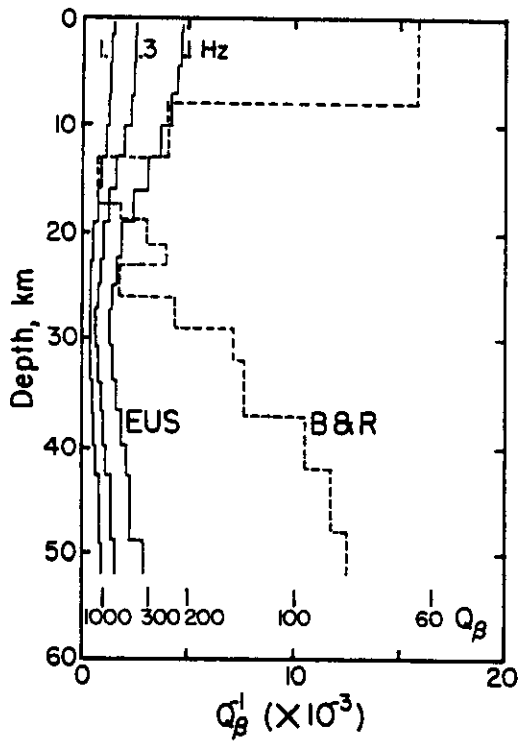

Figure 1

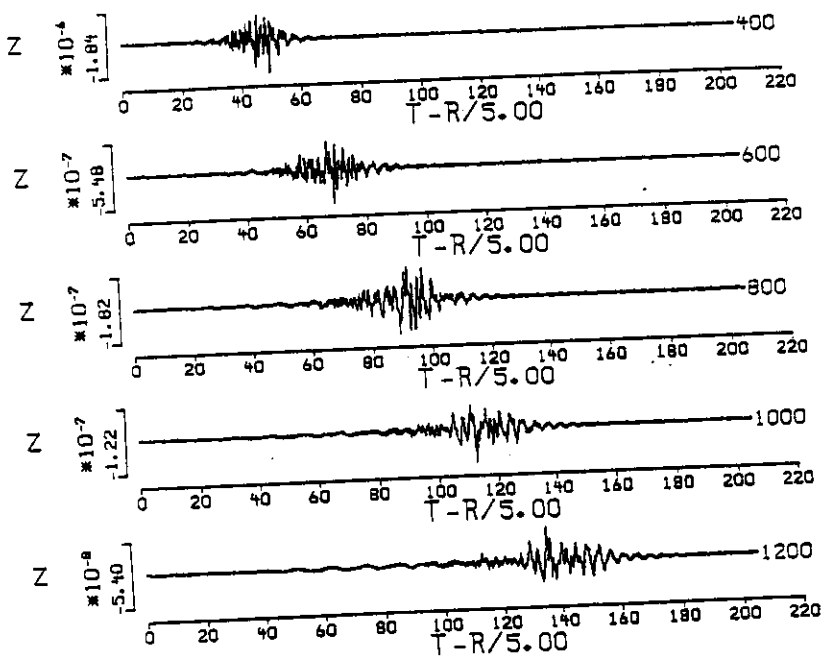

Figure 2

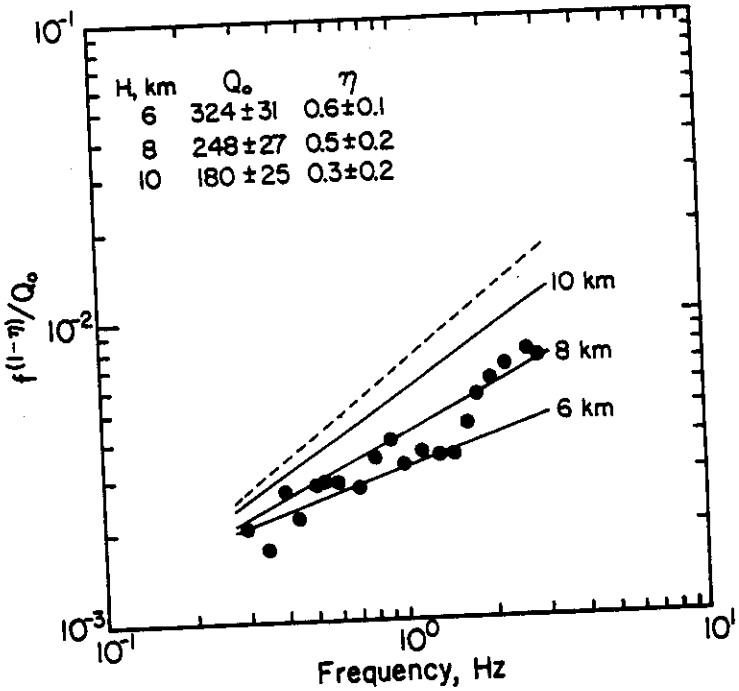

Figure 3

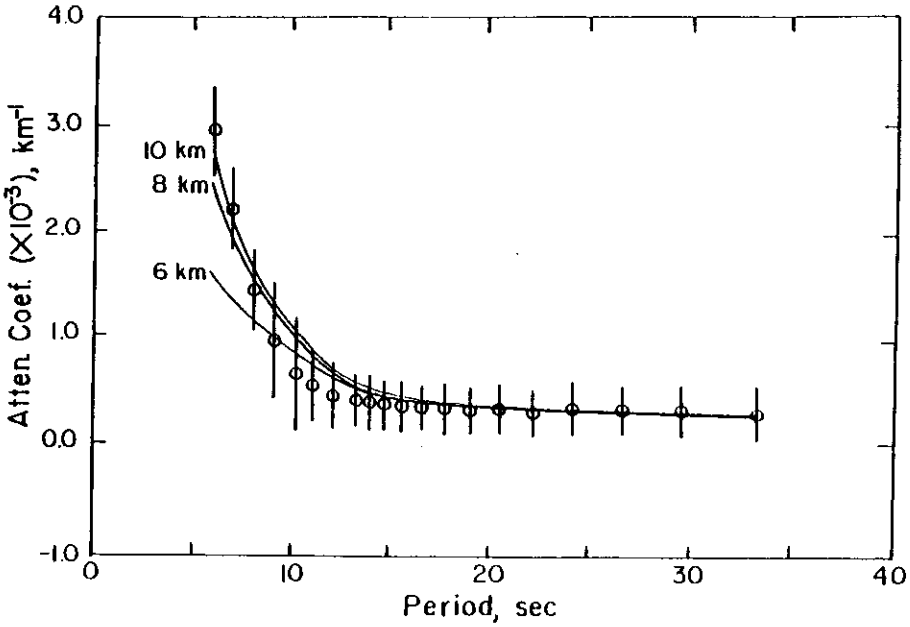
4.0
3.0
2.0
1.0
0.0
-1.0
Atten. Coef. (X10⁻³), km⁻¹
10 km
8 km
6 km
0
10
20
30
40
Period, sec

Figure 4